



**HAL**  
open science

# Monotonic and cyclic tests on beam to column bolted connections with thermal insulation layer

M. Couchaux, A. Alhasawi, A. Ben Larbi

► **To cite this version:**

M. Couchaux, A. Alhasawi, A. Ben Larbi. Monotonic and cyclic tests on beam to column bolted connections with thermal insulation layer. *Engineering Structures*, 2020, 204, pp.109621 -. 10.1016/j.engstruct.2019.109621 . hal-03488568

**HAL Id: hal-03488568**

**<https://hal.science/hal-03488568>**

Submitted on 7 Mar 2022

**HAL** is a multi-disciplinary open access archive for the deposit and dissemination of scientific research documents, whether they are published or not. The documents may come from teaching and research institutions in France or abroad, or from public or private research centers.

L'archive ouverte pluridisciplinaire **HAL**, est destinée au dépôt et à la diffusion de documents scientifiques de niveau recherche, publiés ou non, émanant des établissements d'enseignement et de recherche français ou étrangers, des laboratoires publics ou privés.



Distributed under a Creative Commons Attribution - NonCommercial 4.0 International License

# Monotonic and cyclic tests on beam to column bolted connections with thermal insulation layer

M. Couchaux<sup>a</sup>, A. Alhasawi<sup>a</sup> and A. Ben Larbi<sup>b</sup>

<sup>a</sup> *Institut National des Sciences Appliquées de Rennes, 20 Avenue des Buttes de Coësmes, 35708, Rennes, France*

<sup>b</sup> *Centre Technique Industriel de la Construction Métallique, Espace technologique L'orme des merisiers, Immeuble Apollo, 91193 Saint-Aubin, France*

## Abstract

This paper deals with the mechanical performances of bolted connections with intermediate thermal insulation layer **used** to attach an external steel structure (balconies, passageways) to a steel facade. In the proposed solution, thermal **bridging** is significantly limited by inserting a PVC or plywood plate between an end-plate connection and a steel column. Static and cyclic tests are performed on a cantilever beam connected to a steel column in order to investigate the effect of the thermal insulation layer on the rotational stiffness, bending moment resistances and failure modes. These tests highlight that both the thermal insulation layer and the bolt arrangement (extended and flush end-plate, stiffeners, RHS or I profile) have a significant influence of the connection response.

**Keywords:** *Building; thermal performances; steel structure; thermal break; analytical model; mechanical tests*

## 1 Introduction

The introduction of new energy efficiency standards has pushed the building industry to develop innovative solutions for internally and externally insulated buildings. Systems are thus designed to maintain continuity of the insulation in structural connections while ensuring the transfer of forces. Although improving thermal performances of the envelope components seems attainable goals, the problem of singular points and interfaces between materials need to be solved. The case of thermal breaks that must meet thermal, mechanical and often acoustic performance requirements is a good example.

In recent years, many **research studies** have been conducted to develop solutions to reduce thermal bridging in concrete buildings ([1], [2], [3]). Most of these researches concern linear thermal bridges, mainly at the junctions between the elements of the building envelope. Limited research effort has been devoted to pointwise thermal bridges resulting from connections of systems (solar panels, balconies, passageways) to a façade or roof of a building. Recent research works have been carried out on the mechanical behaviour of connections in steel structures using “insulation” intermediate layers as thermal breaks. Nasdala et al [4] and Sulcova et al [5] proposed to adapt the component method of Eurocode 3 in order to take into account the influence of deformable insulation layers. The results based on numerical simulations [4] showed that the thickness of insulation layer, the friction coefficient at the steel-insulation interface and the initial bolt preload greatly influence the mechanical behaviour of these connections. Cleary et al [6] conducted tests on steel connections using filler plates made of Fiber-Reinforced Resin as thermal barrier. Simple connections and moment connections tested under service loading showed that the thermal filler plates increase the rotation of moment connections and the vertical displacement of simple connections. Peterman et al [7] performed tests on connections insulated by Fiber-reinforced polymer fillers to characterize their long term behaviour and to evaluate the modification of the shear resistance of bolts in presence of fillers. Indeed, fillers induce a bending moment in the bolts in addition to the shear forces and as a result reduce the shear resistance. Ben Larbi et al [9] proposed a thermal break with end-plate connection for external steel structures (balconies, passageways) attached to a concrete façade with

external thermal insulation. This solution consists in the inserting of a rigid PVC plate and an acoustic insulation layer between the end-plate and the support (floor slab, concrete wall). In this case, the end-plate connection needs to be rigid or semi-rigid to fulfil its mechanical function. This simple solution reduces by 20 to 65% the thermal bridge at the connections. Hamel and White [10] performed thermal and mechanical tests on thermal break composed of extended end-plates resting on neoprene and connected to a steel support. The use of neoprene as thermal break clearly decrease the rotational stiffness of the connection and favour the failure of bolts in tension and as a result the ultimate resistance is reduced. The crushing of the neoprene in the compressive area was very important and similar behaviour was observed during tests of Ben Larbi et al [9] on connections with elastomer associated with a PVC. Thus, the use of thermal insulation layers stiffer than elastomer such as PVC and plywood is necessary. Moreover, the compressive area produced by the bending moment being an important source of flexibility, it should be increased and the type of end-plate used will also play an important role in the final rigidity/resistance of the connection.

The behaviour of bolted end plate connections of beam to column under seismic action have been widely studied during the last decades ([11], [12], [13]). The capacity of bolted end-plate connections to dissipate energy is strongly dependent on the bolt configuration [11] and the relative dimensions of the plate and bolts ([11], [12]). Flush end-plate connections are prone to important pinching during cyclic loading ([11], [12]) as a consequence of the absence of contact between the end-plate and the column in the compressive area and also permanent bolt elongation at unloading. Piluso and Rizzano [14] highlighted this pinching effect for T-stubs subjected to cyclic loading. Thermal break attached to steel structures have never been tested under cyclic loadings. The effect of the addition of a thermal insulation layer on the cyclic loading of bolted end-plate connections should be investigated.

This paper presents an experimental study of thermal breaks composed of PVC or plywood layers placed between the bolted end-plate of a steel beam and a support composed of a steel column. The objective of the tests, the experimental test set-up and the mechanical characteristics of materials are presented in section 2. The results obtained during monotonic tests performed on a cantilever beam subjected to a major bending moment and a minor shear force are given in section 3. The effect of

bolt arrangement, thermal insulation on the rotational stiffness and failure mode are highlighted. The image correlation is also used to evaluate the deformed shape of the flanges during the loading and to estimate the area of the compressive zone. Finally cyclic tests have been performed on these configurations (see section 4) to estimate the effect of seismic loading on the deterioration of the mechanical properties of these connections.

## 2 Test program

### 2.1. Objective of the tests

The aim of the tests was to study the effect of bolt configuration and the type of thermal insulation on the mechanical behaviour of thermal break (rotational stiffness, resistances and failure mode) subjected to a major bending moment and a minor shear force. A total of 25 experimental tests have been conducted on a wide range of thermal breaks in the laboratory of INSA Rennes (see Table 1). A series of 16 connections have been subjected to monotonic loadings whilst the remaining connections were tested under cyclic loading. Six configurations of steel connection have been investigated (from PA-1 to PA-6) comprising end-plate welded either to IPE 200 (PA-1, PA-2 and PA-5) or tubes (RHS for PA-3 and PA-4, SHS for PA-6) allowing to evaluate the effect of the beam-shape on the connection's behaviour. The details of the connections are depicted in Figure 1.

**Table 1 : Tested specimens**

Connection	Beam	$t_a$ (mm)	Thermal insulation	Stiffener	Test
PA-1	IPE200	-	-	No	Monotonic/cyclic
RTPA-1-P	IPE200	20	PVC	No	Monotonic/cyclic
RTPA-1-B	IPE200	30	Wood	No	Monotonic/cyclic
PA-2	IPE200	-	-	No	Monotonic/cyclic
RTPA-2-P	IPE200	20	PVC	No	Monotonic/cyclic
RTPA-2-P1	IPE200	10	PVC	No	Monotonic/cyclic
RTPA-2-B	IPE200	30	Wood	No	Monotonic/cyclic
PA-3	RHS 200×120×6	-	-	No	Monotonic
RTPA-3-P	RHS 200×120×6	20	PVC	No	Monotonic
RTPA-3-B	RHS 200×120×6	30	Wood	No	Monotonic
PA-4	RHS 200×120×6	-	-	Yes	Monotonic
RTPA-4-P	RHS 200×120×6	20	PVC	Yes	Monotonic/cyclic
RTPA-4-B	RHS 200×120×6	30	Wood	Yes	Monotonic
RTPA-5-P	IPE200	20	PVC	Yes	Monotonic/cyclic
PA-6	SHS 80×5	-	-	No	Monotonic
RTPA-6-P1	SHS 80×5	10	PVC	No	Monotonic

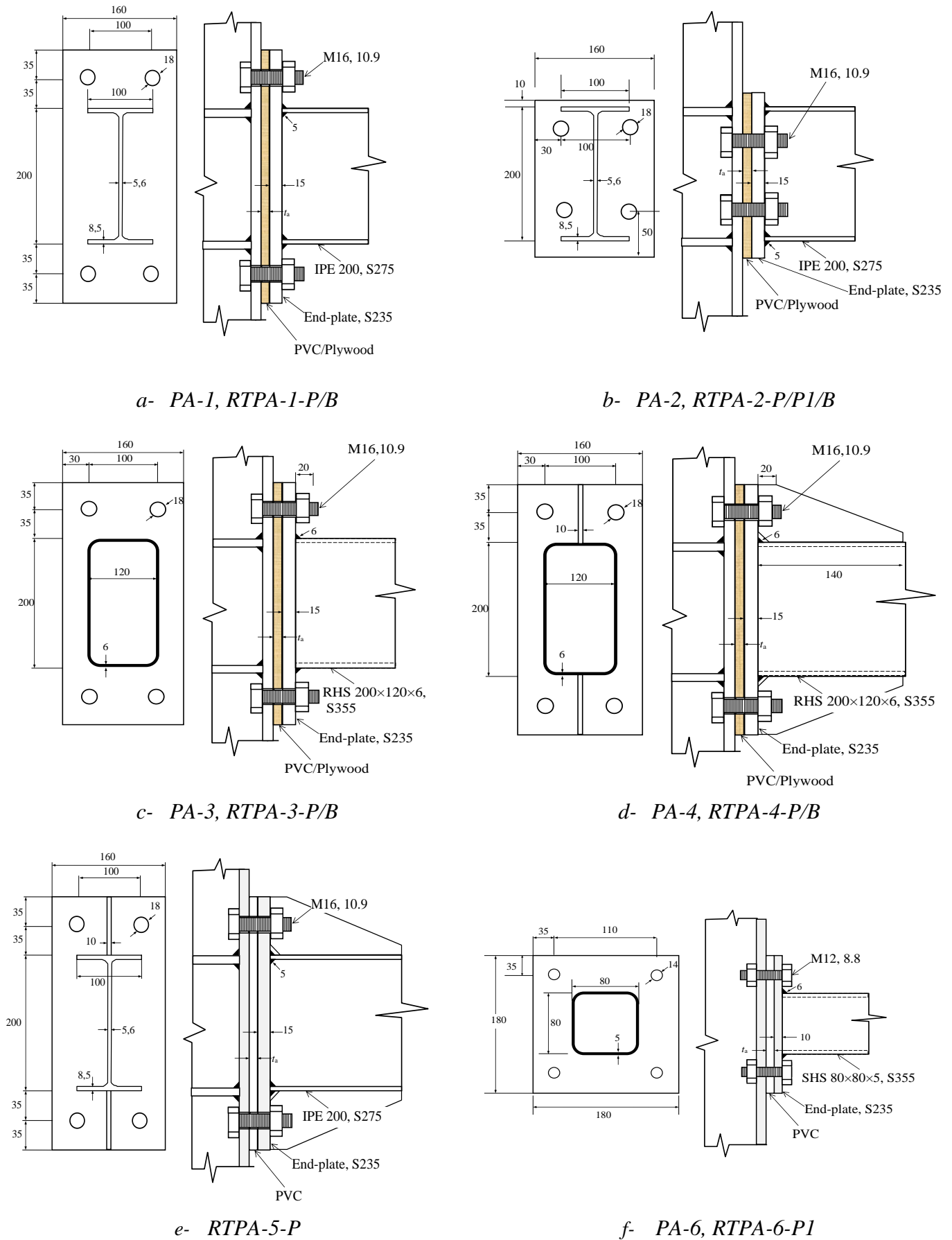


Figure 1 : Geometry of thermal break tested (dimensions in mm)

Specimens PA-1, RTPA-1-P/B and PA-3, RTPA-3-P/B are extended end-plate of 15 mm thickness connected to IPE and RHS, respectively. The connections are designed to favour bolt failure in tension and yielding of the flange in bending (mode 2 according to EN 1993-1-8 [15]). To improve their rotational stiffness and bending resistance, some specimens have been reinforced by stiffeners in the tensile and the compressive area. The aforementioned specimens, for both IPE and RHS, correspond to PA-4, RTPA-4-P/B and RTPA-5-P, respectively.

In addition, specimens PA-2, RTPA-2-P/P1/B are made of flush end-plate to investigate the impact of insulations on these short connections. These beams can potentially be used in balcony or passageways. Furthermore, thermal break could be employed to install elements on the building roof using small dimensions of SHS; specimens PA-6, RTPA-6-P1 are suitable solutions of thermal breaks for these elements. The steel grade of the IPE and tubes are respectively S275 and S355 whereas S235 is used for the end-plate. The bolts used for specimens PA-1 to PA-5 and PA-6 were HR M16 class 10.9 and M12 class 8.8, respectively. The material used for the thermal insulation layer are structural pine plywood or PVC. The thickness of the PVC plate is 10 or 20 mm and that of plywood is 30 mm. The thickness of plywood is larger due to its higher thermal conductivity comparatively to PVC.

### *2.2. Tests set-up*

The test set-up is composed of a cantilever beam connected to a strong column designed to remain elastic during all the campaign test (see Figure 2). The column is braced by a diagonal made of an HEA 200. Lateral supports are placed at mid-length of the beam in order to avoid/delay the lateral torsional buckling of the steel profile. The specimen is loaded by one load-jack with a capacity of 1000 kN in both direction positioned at 1100 mm from the connection. The beam and the insulating layer are replaced after each test. The loading procedures are described for monotonic and cyclic tests in sections 3 and 4, respectively.

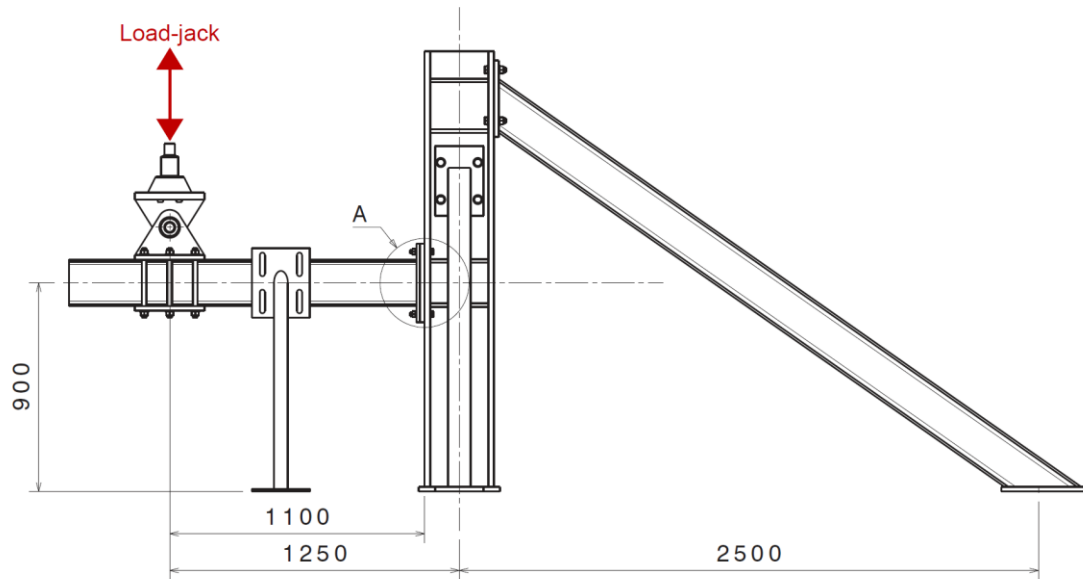


**Figure 2 – Test set-up**

### 2.3. Measurements

Displacement transducers (LVDT) are positioned to measure the displacements at different locations of the test specimen as shown in Figure 3. The horizontal displacement transducers  $U_{t1}$  and  $U_{b1}$  provide a direct estimation of the connection rotation. Inclinometers were also positioned on the beam near the end-plate and on the column in order to evaluate the rotation of the connection. Bolts have been instrumented with axial strain gauges BTM-6C in order to measure the axial strain and thus by calibration, the tensile force in the bolts. Instrumenting the bolts allowed us to control the bolt preload during tightening.

Digital image correlation was used to evaluate the displacements of the end-plates, beam and column in order to determine the rotation of the connection as the deformation of the end-plate relatively to the column. This application is based on the comparison between two images taken at different stages whilst the connection is deforming. One of these images is referred as reference image and the other as deformed image. Targets consisting of black squares with a white fill and a small black dot at the center were affixed to the surface of connections plates and the structural members as shown in Figure 4. The purpose of this tool is to reduce the computational time and to increase the accuracy of the measurements. At the end of the experimental test, all images are uploaded to image

correlation software GOM for analysis. The displacements in the x- and y-direction are determined at the targets by creating face points at its positions on the end-plate and column flange.

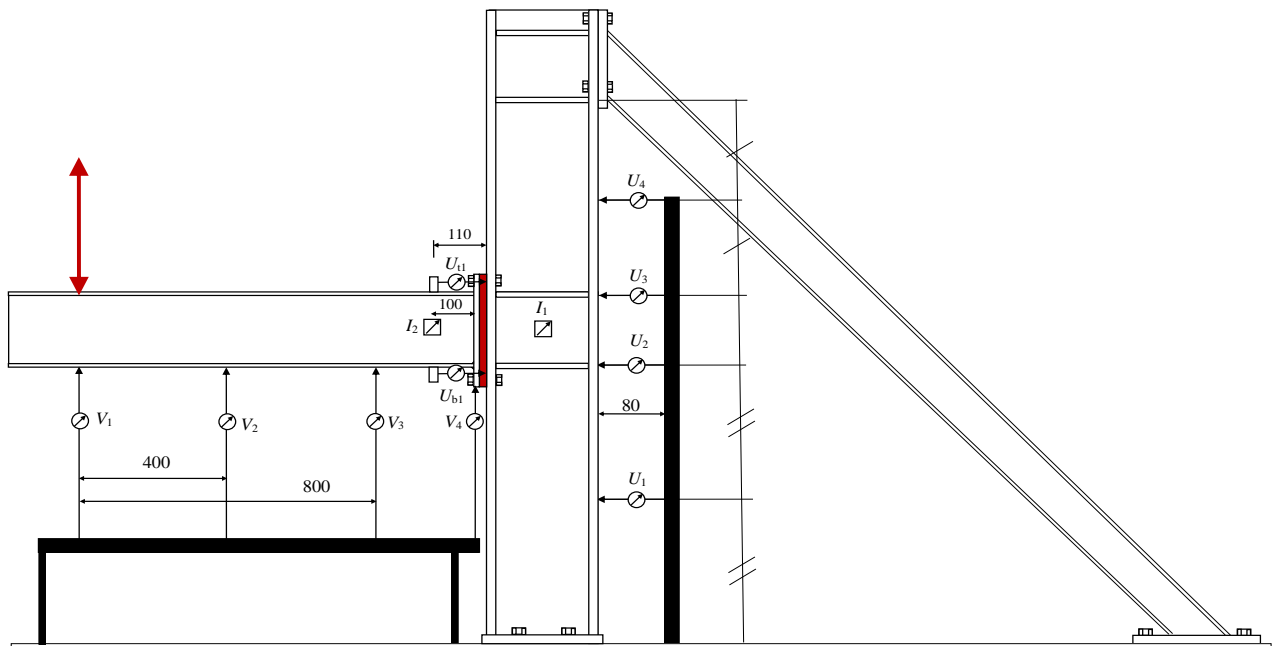


*Figure 3 – Displacements transducers and inclinometers*

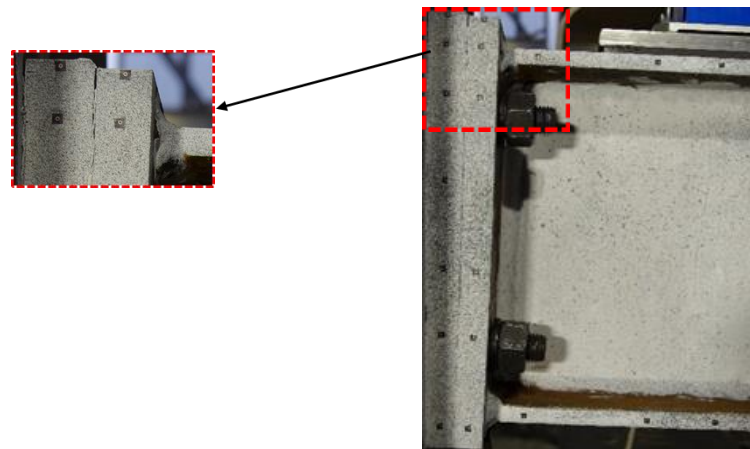


*Figure 4 – Speckle pattern and **target** used for image correlation*

## 2.4. Tests on base materials

### 2.4.1. Mechanical characteristics of steel

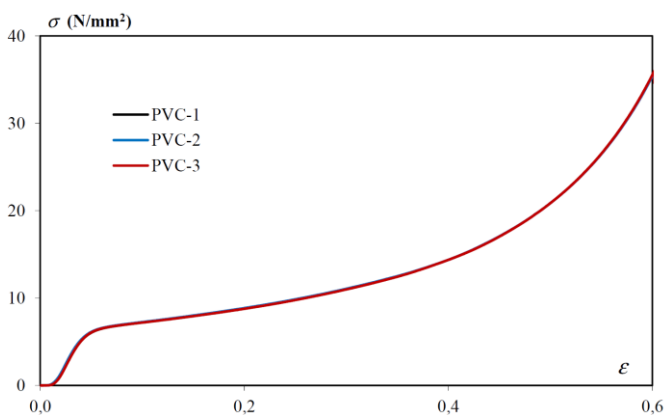
Tests have been performed on coupon extracted from end-plates, IPE/RHS profiles and bolts. The average mechanical characteristics are listed in Table 2.

**Table 2** Average mechanical characteristics of steel

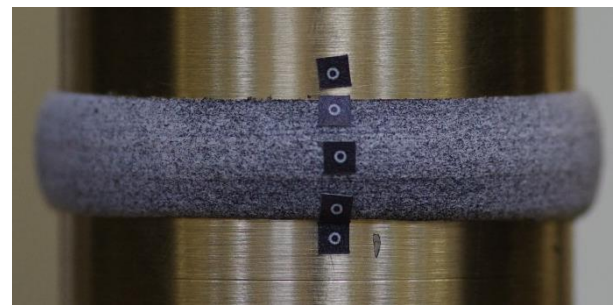
Element	Grade/class	Yield strength	Tensile strength	Elongation for tensile strength	Necking
	-	N/mm <sup>2</sup>	N/mm <sup>2</sup>	%	%
End-plate 10	S235	247	329	26,0	74,4
End-plate 15	S235	331	452	18,3	69,8
IPE200-flange	S275	300	427	20,3	68,2
IPE200-web	S275	307	433	21,7	70,6
RHS200-flange	S355	474	568	14,3	63,4
RHS200-web	S355	486	565	14,7	61,3
SHS 80	S355	514	550	21,3	64,9
Bolt M16	10.9	1025	1117	4,4	76,3
Bolt M12	8.8	813	923	-	61,6

#### 2.4.2. Mechanical characteristics of plywood and PVC

Cylinders of 50 mm diameter made of PVC and plywood have been tested in compression (see Figure 5 and Figure 6). For the two materials, the behaviour is elastic for stress lower than 5-6 N/mm<sup>2</sup> and become elasto-plastic for higher stress values with a hardening, producing large permanent strains. The yield strength of PVC and plywood material are equal to 4,4 and 6 N/mm<sup>2</sup>, respectively. The Young Modulus of PVC and plywood material are equal to 200 and 302 N/mm<sup>2</sup>, respectively. These values are very low comparatively to that of steel and will constitute the flexible part of the connection in the compression area and in the tensile area for the prying force.

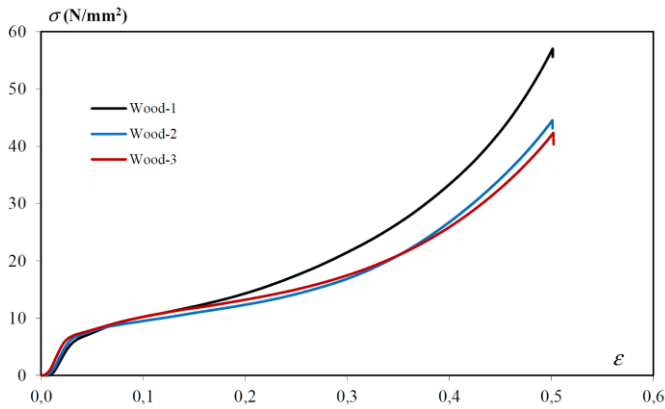


a- Stress-strain curve

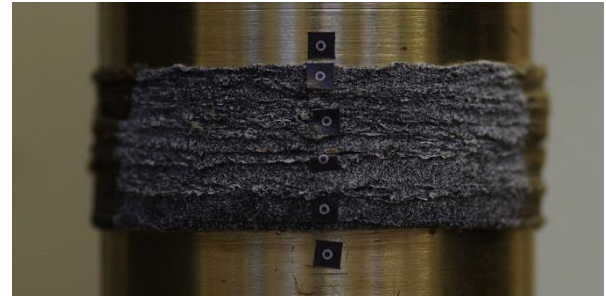


b- PVC cylinder at the end of test

**Figure 5** : Compression tests on PVC



a- Stress-strain curve



b- Plywood cylinder at the end of test

**Figure 6 : Compression tests on plywood**

### 3 Monotonic tests

#### 3.1. Loading procedure

To estimate the influence of preloaded bolts on the evolution of the bolt forces and the rotational stiffness, the connections were initially tested in the elastic regime for two levels of bolt tightening as presented in Table 3. All bolts were instrumented, so that tightening was performed by reading the strain gauge according to the calibration factor. The two loading cycles, each one corresponding to a level of preloading, are labelled stage 1 and 2. In presence of thermal insulating layer, the bolt preloading was equal to 25 kN during stage 1 and 50 kN during stage 2. However, the bolts in conventional connections (without thermal insulation layer) were preloaded with a constant force of 30 kN in stage 1 and with a varying force between 60 and 110 kN in stage 2. The objective of this last stage was to apply the nominal preloading according to EN 1090-2 [16]. Some bolts were not able to reach the nominal preloading due to the modification of the friction coefficient of fillet during the process of instrumentation. After these two elastic cycles, HR instrumented bolts are removed (except one) and replaced by non-instrumented bolts. To evaluate the plastic and ultimate resistances of the connections, the bolts were snug-tightened and a bending moment was applied until the failure. It is worth to mention that in all tests force-control loading conditions were applied in the elastic regime. In the elasto-plastic regime, displacement control loading conditions were adopted.

**Table 3 : Bolt preloading during stage 1 and 2**

Specimen	$B_{01}$	$B_{02}$
	kN	kN
PA-1	30	110
RTPA-1-P	25	50
RTPA-1-B	25	50
PA-2	30	70
RTPA-2-P	25	-
RTPA-2-P1	25	-
RTPA-2-B	25	50
PA-3	30	60
RTPA-3-P	25	50
RTPA-3-B	25	50
PA-4	30	60
RTPA-4-B	25	50
RTPA-4-P	25	50
RTPA-5-P	25	50

### 3.2. Moment rotation-curve and failure modes

The moment-rotation curves of connections obtained for different specimens during stage 3 are presented in Figure 8. The rotation of the connection,  $\theta_{c,U}$ , is obtained from horizontal LVDT,  $U_{t1}$  and  $U_{b1}$ . Furthermore, from the aforementioned curves, the following parameters are extracted and provided in Table 4:

- the **secant rotational stiffness** evaluated for  $2/3M_{j,pl}$ ,
- the **plastic bending resistance**  $M_{j,pl}$  calculated according to ECCS requirements [17] that corresponds to the frontier between the elastic and elasto-plastic range of behaviour,
- the **ultimate bending resistance**  $M_{j,u}$  corresponding to the maximum bending moment applied during tests,
- elements that yield/crack before failure and the **failure mode**.

Most of specimens, except for thermal breaks attached to RHS without stiffeners, failed by bolt ruptures in tension (see Figure 7-a). For specimens RTPA-3-P/B, PA-6 and RTPA-6-P1 failure is due to weld tearing at the corner (see Figure 7-b) after major bending of the end-plate. Excluding the specimens PA-3, the additional thermal insulation layer do not influence the failure mode. For specimens PA-3, the single fillet weld that attach the end-plate to the tube is bent until tearing. The additional insulating layer increases this phenomena.



a- Bolt rupture in tension



b- Weld tearing

**Figure 7 : Failure modes for monotonic tests**

Specimen	$S_j$	$M_{j,pl}$	$M_{j,u}$	Failure mode	Yielding/cracking
	kNm/rad	kNm	kNm		
PA-1	9880	44,6	73,8	Bolt	Bolt, flange
RTPA-1-P	8106	32,6	66,6	Bolt	Bolt, flange, PVC
RTPA-1-B	8624	34,8	71,2	Bolt	Bolt, flange, plywood
PA-2	10195	40,0	60,7	Bolt	Bolt, flange
RTPA-2-P	2880	12,2	50,4	Bolt	Bolt, PVC
RTPA-2-P1	3196	29,2	50,7	Bolt	Bolt, flange, PVC
RTPA-2-B	4266	15,4	48,1	Bolt	Bolt, plywood
PA-3	16860	32,8	67,6	Bolt	Bolt, flange
RTPA-3-P	6540	38,2	66,4	Weld	Bolt, weld, flange, PVC
RTPA-3-B	6364	41,0	58,5	Weld	Bolt, weld, flange, plywood
PA-4	19000	57,0	88,8	Bolt	Bolt, flange, weld
RTPA-4-P	12914	42,7	85,0	Bolt	Bolt, flange, PVC
RTPA-4-B	11973	44,5	85,0	Bolt	Bolt, flange, plywood
RTPA-5-P	13343	42,1	79,5	Bolt	Bolt, flange, PVC, weld
PA-6	1425	7,5	14,6	Weld <sup>(1)</sup>	Bolt, weld, flange
RTPA-6-P1	705	8,0	15,1	Weld <sup>(1)</sup>	Bolt, weld, flange, PVC

Note 1 : The test was stopped after major vertical displacements

**Table 4 : Bending resistances and failure modes for monotonic tests**

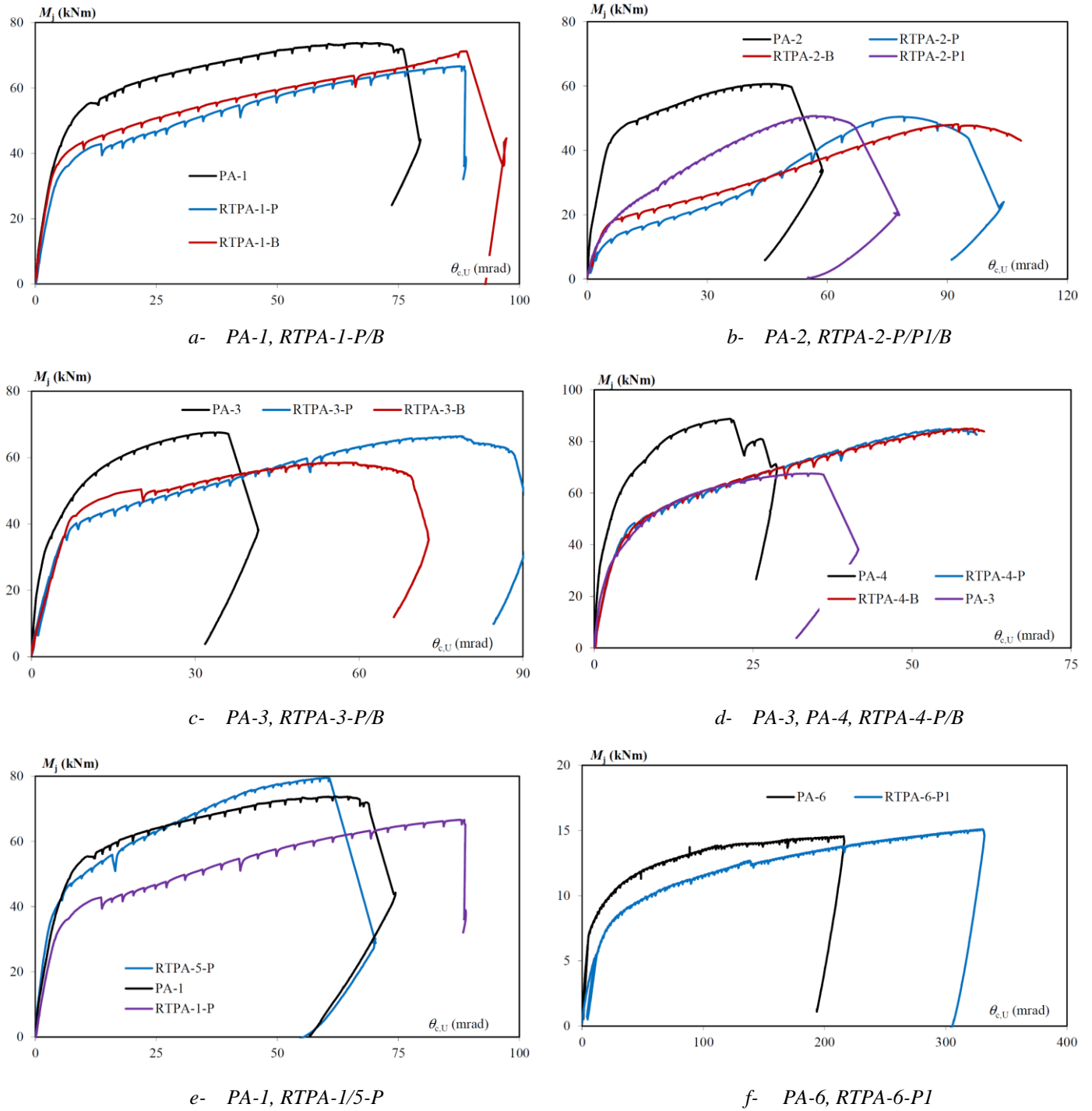
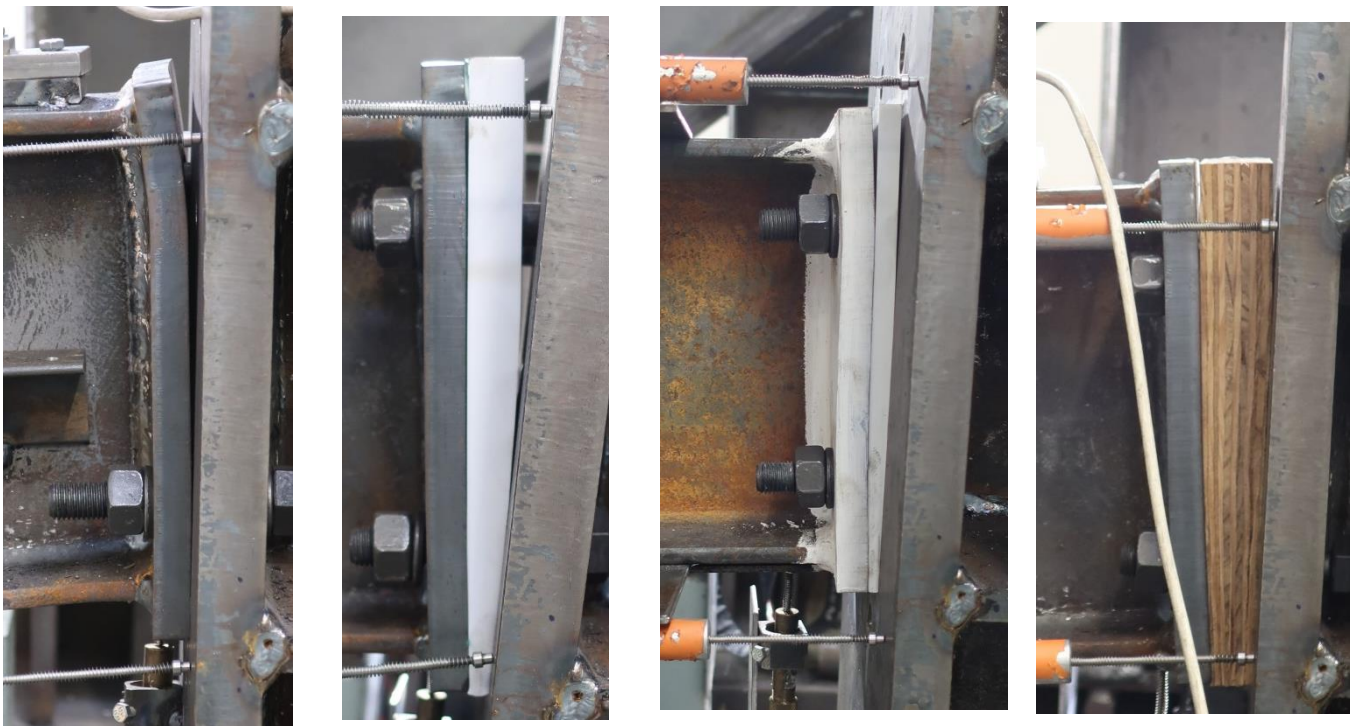


**Figure 8 – Moment-rotation curves during monotonic tests**

For specimens RTPA-1-P/B, the ductility is slightly increased (see Figure 8-a) comparatively to PA-1 due to crushing of the thermal insulation. The behaviour of PA-1 and RTA-1-P/B are quite similar except that the non-linear behaviour starts earlier. The secant rotational stiffness decreases by 18 % and 13 % in presence of PVC and plywood, respectively. The deformed shapes of specimens PA-1 and RTPA-1-P/B at failure are presented in Figure 9. For the three specimens, the flange yields in bending in the tensile area and a yield line parallel to the beam flange develops. For PA-1, the prying force seems to be positioned at the outer edge of the flange whereas for specimens with thermal break the contact area extends between the free edge of the end-plate and the bolts. These observations will be confirmed by results of image correlation (see section 3.4). An important crushing of the plywood and PVC is obtained at failure and contact area extends from the extended end-plate to a portion of the beam web. In absence of thermal break, the compression area only develop at the bottom of the extended end-plate. The use of PVC and plywood decreases the ultimate bending moment by 9,7% and 3,5 %, respectively. This difference is mainly due to the fact that the use of a flexible thermal insulation layer increase the size of the compressive area and also decrease the lever arm. However, it is worth to mention that the resistance of bolts in tension depends on the length of the threaded area which is enlarged here by the use of thermal insulation. The decrease of the plastic bending moment is more significant as it is equal to 27 and 22 % in presence of PVC and plywood, respectively. This important decrease is due to yielding of the thermal insulation in compression that appear before yielding of the end-plate in bending.



the increase of the compressive area and thus the reduction of the lever arm. The decrease of the plastic bending moment is significant for specimens RTPA-2-P/B as it is divided by 3-4 comparatively to the conventional connection. For these two specimens, the drop of the plastic bending moment is due to premature yielding of the thermal insulation layer in the compression area. Due to the absence of a bolt row below the lower flange of the beam, the spread of the compressive area is limited and the resistance of PVC and plywood is rapidly reached. The use of a 10 mm thickness PVC really improve the results as the plastic bending moment decreases only by 27 % compared to a conventional design.



*a- PA-2*

*b- RTPA-2-P*

*c- RTPA-2-P1*

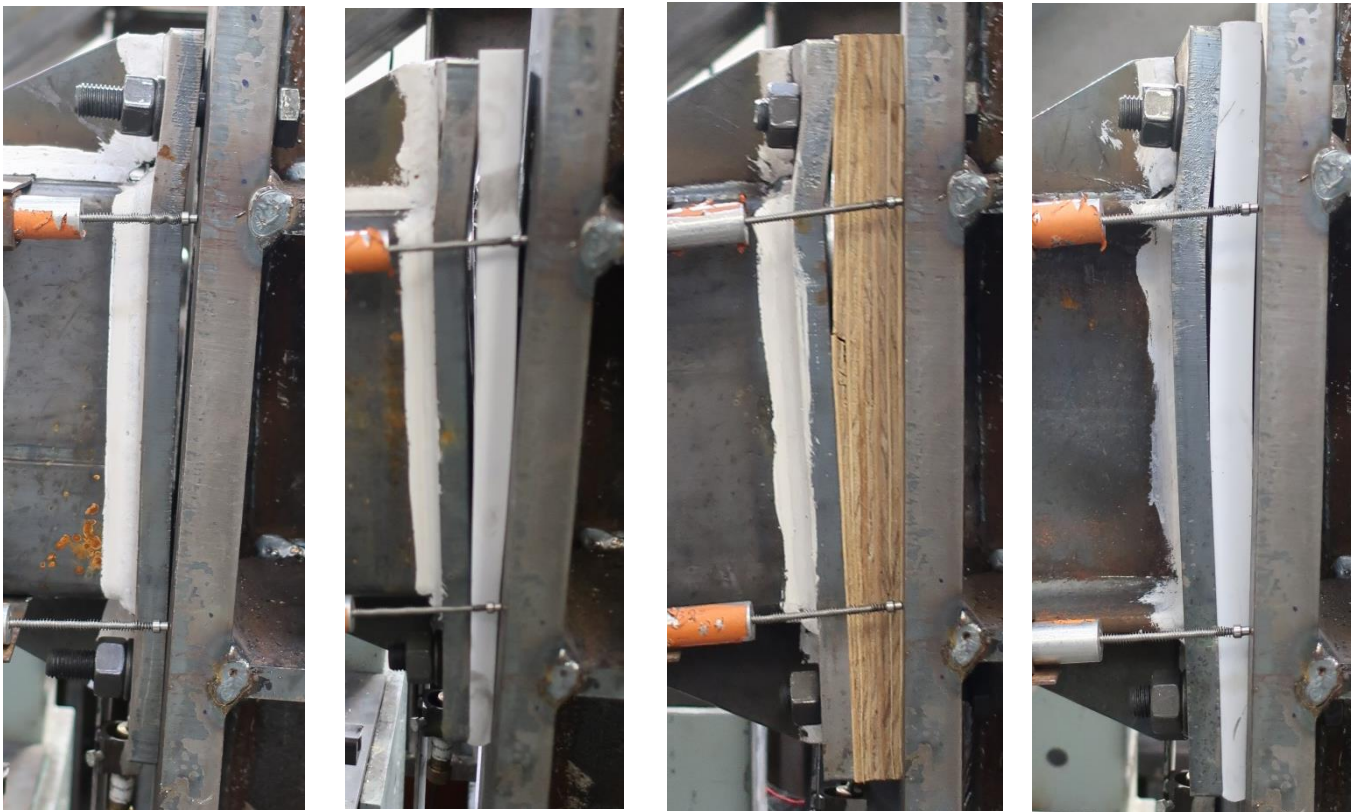
*d- RTPA-2-B*

**Figure 10** – Deformed shape of specimens PA-2, RTPA-2-P/P1/B at failure

For specimens RTPA-3-P/B, the secant rotational stiffness is divided by 2 comparatively to specimen PA-3 (see Table 4). The rotation capacity is increased in presence of thermal insulation layer due to its flexibility (see Figure 8-c). The deformed shapes of specimens PA-3 and RTPA-3-P/B at failure depicted in Figure 11 are similar to those of PA-1 and RTPA-1-P/B. Again, a plastic yield line develops in the end-plate, in the tensile area. Due to prying effect, an important crushing of the PVC and plywood develops in both the compressive area and the tensile part. The crushing is more pronounced in presence of PVC. The failure of these specimens have been obtained by weld tearing



tensile area and a final bolt rupture in tension lead to connection failure. The behaviour of connections of RHS is clearly improved comparatively to specimens RTPA-3-P/B as no weld tearing has been observed. Weld cracks in the most stressed area were observed but their propagation was limited. For specimen with RHS, the use of thermal insulating layer decrease the ultimate resistance only by 4,3%. The decrease of the plastic bending moment ranging between 22 and 25 %, is more significant and due to yielding of the thermal insulation in compression. The use of stiffeners increases the resistances of the specimens that use thermal insulation layer and permit to obtain stiffness and bending resistances close to the same specimen without thermal insulation layer and stiffeners.



*a- PA-4*

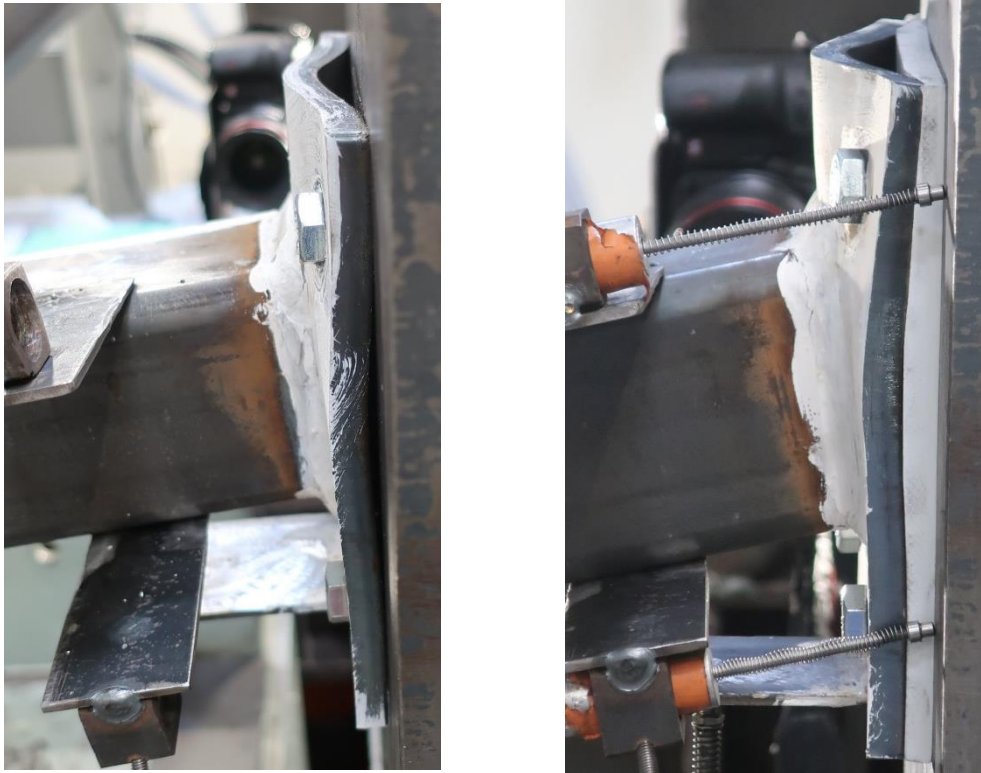
*b- RTPA-4-P*

*c- RTPA-4-B*

*d- RTPA-5-P*

**Figure 12** – Deformed shape of specimens PA-4, RTPA-4-P/B and RTPA-5-P at failure

The deformed shape of specimens PA-6 and RTPA-6-P1 at the end of the test are depicted in Figure 13. Extensive yielding of the flanges has been observed for the two specimens with crushing of the PVC in the compressive and the tensile areas. The secant rotational stiffness of RTPA-6-P1 is divided by 2 comparatively to PA-6. The addition of thermal insulation don't modify the plastic bending resistance as the first yielding is obtained in the end-plate under bending loading.



*a- PA-6*

*b- RTPA-6-P1*

**Figure 13 – Deformed shape of specimens PA-6 and RTPA-6-P1 at the end of test**

The moment-curves obtained during stages 1, 2 and 3 are depicted in Figure 14 for specimens PA-3 and RTPA-3-P. During these stages, the only difference is the bolt preloading that varies between 10 and 60 kN for the two specimens. For PA-3, the moment rotation curve is clearly sensitive to bolt preloading. Hence at the start of loading, the stiffness is about the same for the three level of preloading. However during stage 1 and 3, the stiffness decrease for a bending moment of about 20 kNm due to the progressive uplift of the flange near bolt head. This decrease of the stiffness is not clearly observed during stage 2 as bolt preloading is sufficient to maintain contact between end-plates behind the bolts. On the contrary, stiffness alteration is not clearly observed with connection RTPA-3-

P and preloading do not have an impact on the rotational stiffness. These results make sense as the preloaded bolt rest on a very flexible support made of PVC or plywood (see section 3.3).

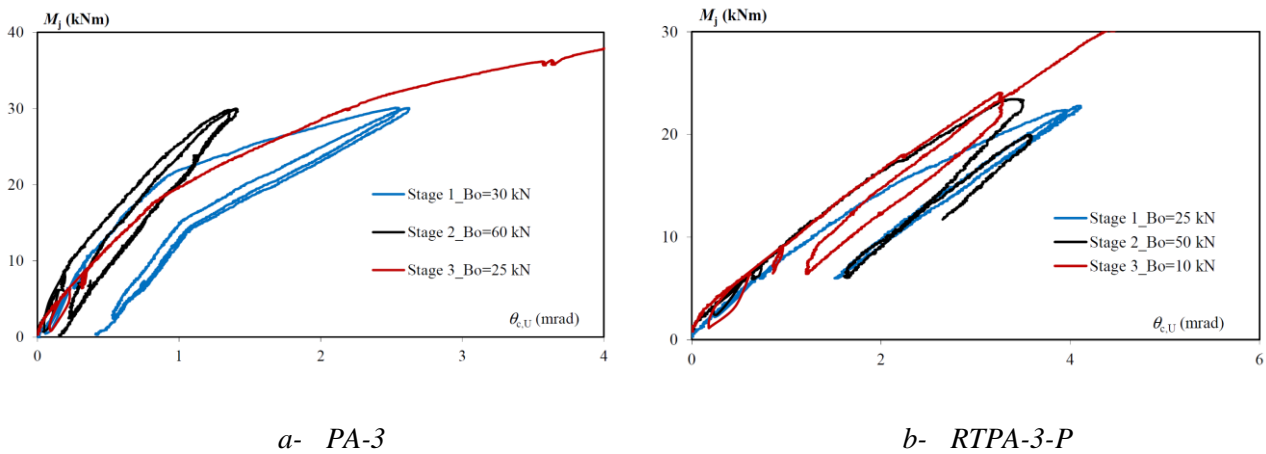
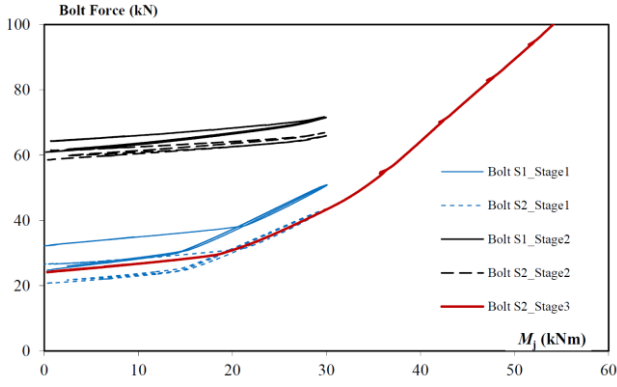


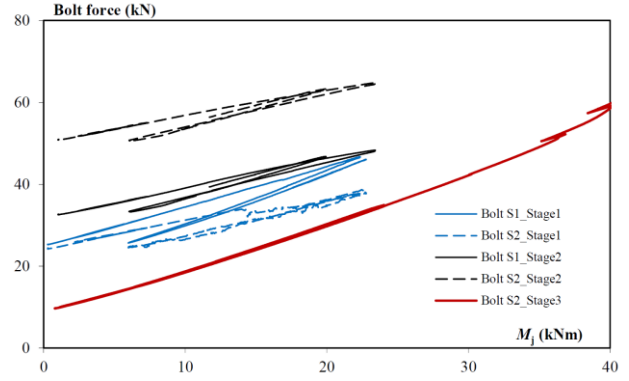
**Figure 14** – Moment-rotation curves during stages 1, 2 and 3

### 3.3. Bolt force

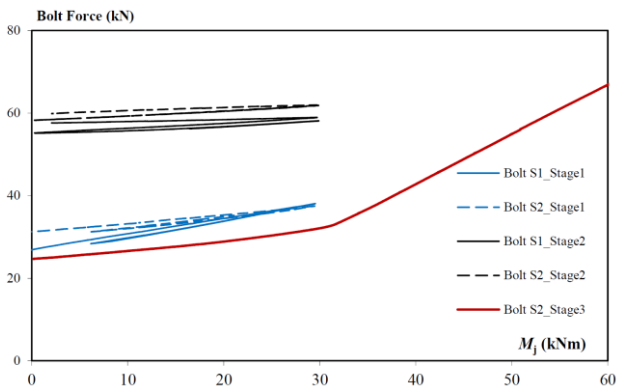
The evolution of bolts forces are presented in Figure 15 as a function of the bending moment applied during stages 1, 2 and 3. For conventional connections PA-3 and PA-4 two classical steps are observed when the applied bending moment is sufficiently large. Firstly, bolt forces remain nearly constant due to initial bolt preloading and the contact area is located essentially below and around the bolt head. With increasing value of the tensile force, the contact area moves towards the free edges producing a rapid increase of the bolt forces. The curve of bolt forces as a function of the bending moment tends to an asymptote. For each stage, the curves tend to parallel asymptotes. The second step is not observed for PA-3 during stage 2 and PA-4 during stages 1 and 2 as preloading was sufficient to maintain the contact around the bolt area. Specimen PA-4 being more rigid than specimen PA-3 uplift occurs later. This two steps does not appear at all in presence of thermal insulation layer.



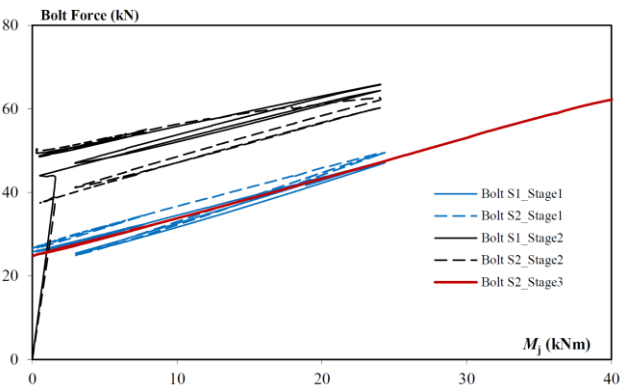
a- PA-3



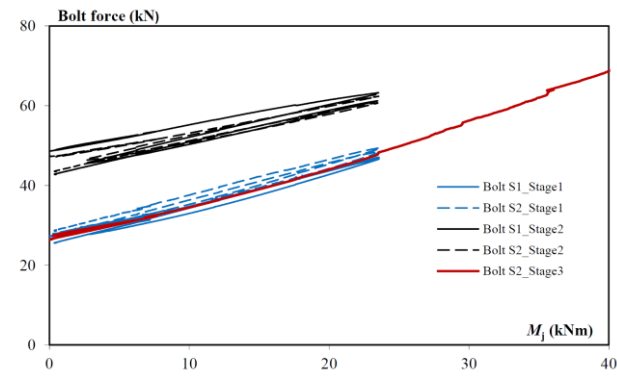
b- RTPA-3-P



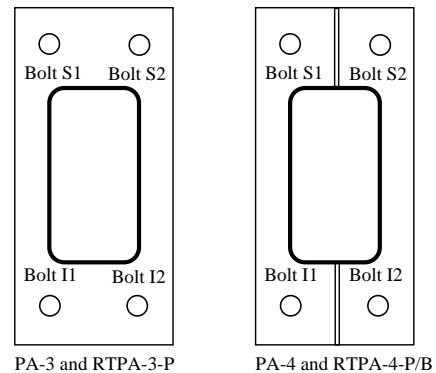
c- PA-4



d- RTPA-4-P



e- RTPA-4-B



f- Bolt configuration

**Figure 15** – Evolution of bolt force during stages 1, 2 and 3

For a preloaded bolted connections the tensile force applied to a bolt,  $F_T$ , leads to the following bolt force:

$$B = B_0 + \left[ \frac{k_b}{k_b + k_c} \right] \lambda F_T \quad (1)$$

where  $k_b$  is the stiffness of the bolt in tension,  $k_c$  the stiffness of the plates with the thermal insulation layer in compression,  $\lambda$  a lever arm factor that consider prying effect and  $B_0$  the initial bolt preloading.

The uplift appears for the following tensile force:

$$F_{T,1} = B_0 \frac{k_c + k_b}{\lambda k_c} \quad (2)$$

The thermal insulation layer being very flexible compared to bolts, the tensile force  $F_{T,1}$  is quite large so stage 1 is mainly observed while the connection behaves elastically. Moreover, the evolution of the bolt force is close to that obtained in absence of preloading as:

$$B \approx B_0 + \lambda F_T \quad (3)$$

Finally, connections with thermal insulating layer are not sensitive to bolt preloading as the rotational stiffness and bolt forces remain unchanged.

The relationship between the bolt forces and the bending moment during stage 3 is presented in Figure 16. For specimens with thermal insulating layer, the slope of the curve is parallel to that obtained with a conventional connection. The non-linear part starts earlier due to yielding of the thermal insulation. For specimen RTPA-2-P, the maximal bolt force is clearly below their tensile resistance equal to 175 kN. This decrease is probably due to the transfer of a significant bending moment by the bolts.

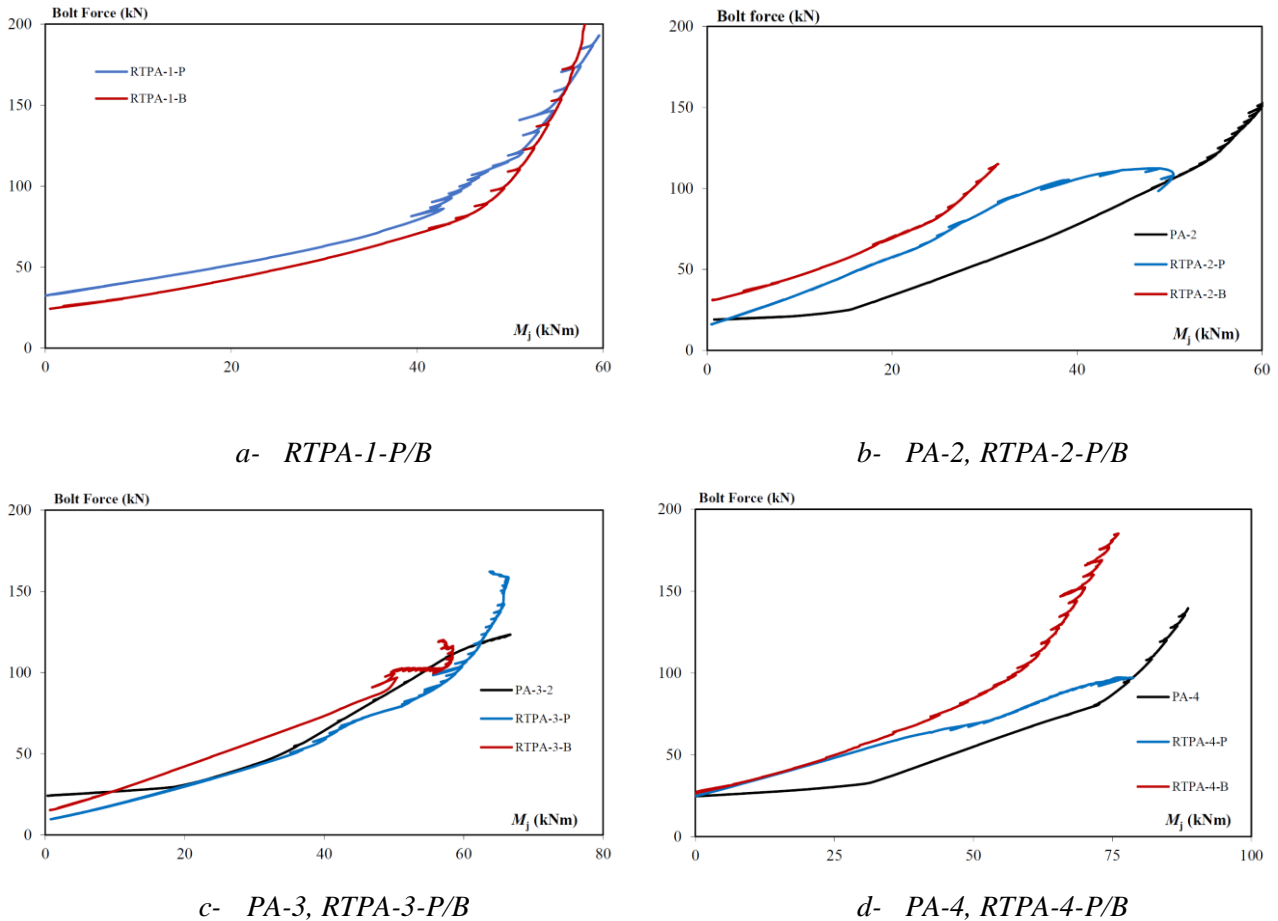


**Figure 16** – Evolution of bolt force until failure

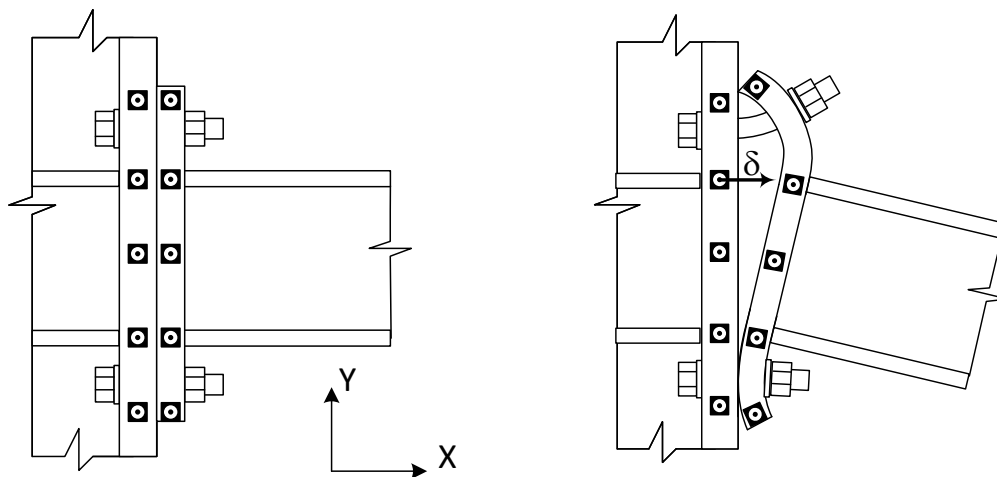
### 3.4. Flange deformation

Image correlation has been used to evaluate the relative displacement between the column flange and the end-plate (see Figure 17) in order to estimate the crushing of the thermal insulation layer and thus the **extent** of the compression area.

The relative displacement between the column flange and the end-plate at failure is depicted in Figure 18 as a function of the position of the target with respect to the bottom of the end-plate. A negative displacement corresponds to a crushing of the thermal insulation whilst a positive one is associated to end-plate uplift. The deformed shape of specimens with and without thermal break are significantly different, particularly the size of the compressive area. For specimen PA-1, the bottom extended end-plate is in contact (see Figure 18-a) and uplift starts in the vicinity of the bottom flange of the beam. For specimens with thermal insulation layer, RTPA-1-P and RTPA-1-B, the compression area extends over 30% of the beam depth. In the compression area, the displacement is not linear. The end-plate is probably bent due the contact pressure that develops. The maximum uplift of the flange is

approximately similar for specimens PA-1, RTPA-1-P/B and is located just below the upper flange of the beam and not at the weld toe. In addition, the contact area resulting from prying effect is different. In the presence of thermal insulating layer an important crushing (5 mm) is observed and the size of the contact area is about 25-30 mm. The thermal insulating layer being flexible, the contact area should extend in order to transfer the prying force. The results obtained with extended end-plate of tubes (see Figure 18–c) are similar to that obtained with I profile.

For flush end-plate connections (see Figure 18–b), the results are completely different. For specimens with thermal insulating layer, the compression develops over half the beam depth. For plywood and PVC of 20 mm thickness, the deformed shape is almost linear even in the tensile area. For specimen PA-2, the compression area cannot be observed. As a result of prying effect, the end-plate is in contact in the vicinity to the bolt. In contrast with extended end-plate connections, the prying action **does** not develop at the upper edge of the end-plate.



a- Reference image

b- Deformed image

**Figure 17** : Evaluation of relative displacement of end-plate and column flange with image correlation

For specimen PA-4, the compression **does** not develop over the entire area of the bottom extended end-plate. The position of the separation point lays between the outer edge of the end-plate and the bottom flange of the beam. In presence of thermal insulation layer, the compression area extends over half the beam depth as for flush end-plate connections. The compression area is **hence** larger with the addition of stiffeners to extended end-plate. **For specimens RTPA-3-P/B**, the compression area **was** limited to 30 % of the beam depth. This difference can be explained by the fact that the tensile part is more rigid in presence of stiffeners which result in a larger compression area. In the upper edge of the

end-plate, the crushing is limited as the stiffeners reduce prying effect in the tensile area. In the compression area, the end-plate remains straight due to the presence of the stiffeners.

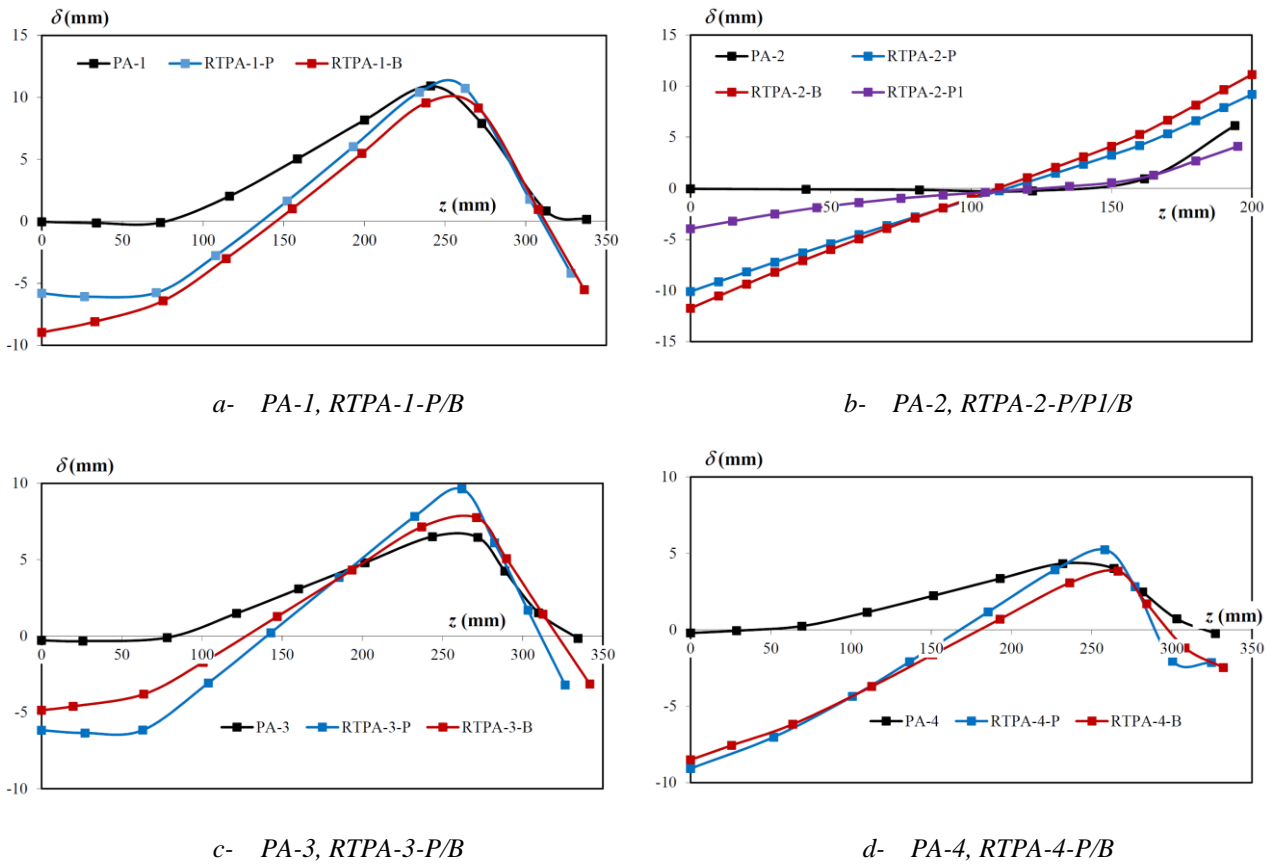


**Figure 18** – Relative displacements of end-plate and column flange at failure

### 3.5. Monotonic tests : concluding remarks

In the present study, the introduction of thermal insulation layer composed of PVC (10 or 20 mm thickness) or plywood (30 mm thickness) decreases the ultimate resistance. For extended end-plate with stiffeners, this decrease is limited, less than 5%. For non-stiffened end-plates, with I or RHS profile, this decrease is less than 13 % in the worst case. For flush end-plate connections, the reduction of resistance goes to 15-20%. The geometry of the end-plate has a clear impact on the resistance particularly concerning the size of the potential compression area that can develop. The thermal insulation layer being flexible compared to steel, a large compression area is needed to equilibrate the tensile force due to the bending moment. In presence of flush end-plate, this compression area is rather limited and the lever arm decreases also. **On the contrary, the stiffeners permit to increase the lever arm and the capacity of the tensile area.** The consequence of the geometry of the end-plate are also important for the rotational stiffness that is divided up to 2 when using thermal insulation layer with

extended end-plate and up to 3 for flush end-plate connections. This decrease is due to the crushing of the thermal insulation layer that is more substantial in case the compression area is reduced.

The plastic bending moment that corresponds to the frontier between the plastic and the elastic behaviour is more sensitive to the presence of thermal insulation layer than the ultimate bending moment. Hence for extended end-plate connections, the decrease of the plastic bending moment is about 20 % whereas for the ultimate bending resistance, the decrease was limited to 10%. For flush end-plate connections, the plastic bending moment is divided by 3 in presence of plywood or PVC of 20 mm thickness. This reduction of the plastic bending moment is mainly caused by yielding in compression of the thermal insulation layer. The use of PVC of 10 mm thickness in presence of flush end-plate connections limits the decrease of stiffness and permit to get a plastic bending moment closer to that obtained without thermal insulation.

The stiffeners improve the mechanical characteristics (rotational stiffness, plastic and ultimate bending moment) as an extended end-plate with stiffeners and thermal insulation layer exhibit the same characteristics as an extended end-plate without stiffeners and thermal insulation layer.

In presence of thermal insulation layer composed of plywood or PVC, bolt preloading do not have a clear effect on the rotational stiffness and the evolution of bolt forces is not modified by the level of preloading. Image correlation demonstrates that the compression area can spread over half of the end-plate length in presence of thermal insulation. For extended end-plate with stiffeners and no thermal insulation, the compression is located at the bottom of the extended end-plate.

## 4 Cyclic tests

### 4.1. Loading procedure

The cyclic tests were performed considering the **European testing procedure for structural elements under cyclic loads, ECCS-45 [17]**, based on the elastic displacement deduced from the previous monotonic tests. Cyclic loading was executed in displacement-controlled manner. Bolts were snug-tightened as it is usually done in practice for structures like balcony, passageway...

### 4.2. Failure modes

The failure modes along with the elements that yield/crack during cyclic tests are listed in Table 5. The maximum bending moments obtained in monotonic and cyclic tests, noted  $M_{j,u,mon}$  and  $M_{j,u,cyclic}$  respectively, are also given in Table 5. Except for specimens PA-1 and RTPA-1-P/B, the failure modes are similar to that observed during static tests and corresponds to bolt failures in tension (see Figure 19-a). For specimen PA-1, failure corresponds to tearing of the weld next to the two flanges (see Figure 19-b) preceded by major end-plate yielding in bending. The addition of a thermal insulation layer as for specimens RTPA-1-P/B leads also to weld tearing but the final failure is due to bolt rupture in tension. These extended end-plates with fillet welds are really sensitive to low-cycle fatigue and the addition of stiffeners for specimens RTPA-4-P and RTPA-5-P modify the final failure modes.

**Table 5 : Bending resistances and failure modes for cyclic tests**

Specimen	$M_{j,u,mon}$ kNm	$M_{j,u,cyclic}$ kNm	Failure mode	Yielding/cracking
PA-1	73,8	74,1	Welds	Bolts, flange, welds
RTPA-1-P	66,6	60,5	Bolts, welds	Bolts, flange, welds, PVC
RTPA-1-B	71,2	62,7	Bolts, welds	Bolts, flange, welds, plywood
PA-2	60,7	55,9	Bolt	Bolt flange
RTPA-2-P	50,4	50,1	Bolts	Bolt, PVC
RTPA-2-P1	50,7	53,2	Bolts	Bolt, PVC, flange
RTPA-2-B	48,1	50,9	Bolts	Bolt, plywood
RTPA-4-P	85	88,0	Bolts	Bolt, flange, PVC, weld
RTPA-5-P	79,5	90,6	Bolts	Bolt, flange, PVC, weld



*a- Bolt rupture in tension*



*b- Weld tearing*

**Figure 19 : Failure modes for cyclic tests**

The maximum bending moment obtained during cyclic tests for specimen PA-1 is close to that of monotonic test. On the contrary, in presence of thermal insulation layer, the resistance decreases by 10 % due to the fact that the outer welds failed. Consequently the lever arm increases and favour bolt rupture in tension. It can be noted that prying effect disappear in the tensile part (see Figure 20-b and c) during cyclic loading due to the permanent deformation in compression of the insulation layer produced by reverse loading. This lack of prying effect, favourable for bolt failure in tension **does not** improve the resistance comparatively to the monotonic tests. The tearing of the welds and the increase of the corresponding lever arm are preponderant for these specimens.



*a- PA-1*



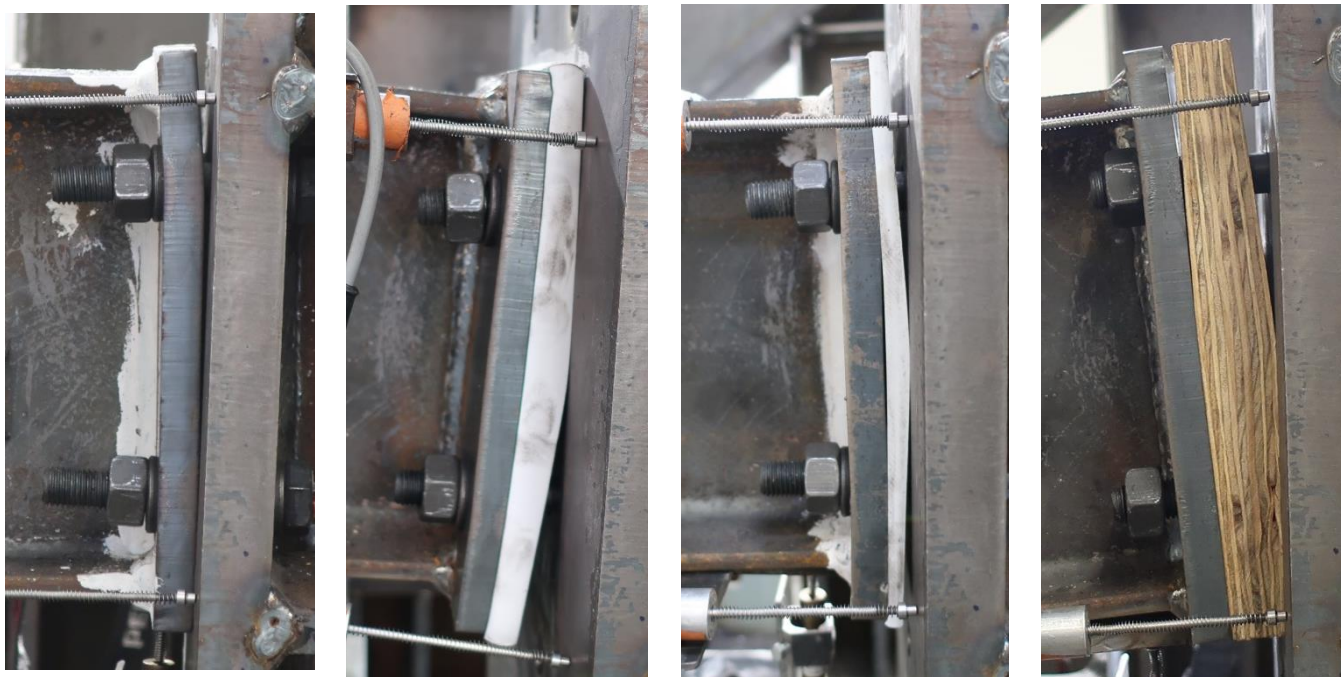
*b- RTPA-1-P*



*c- RTPA-1-B*

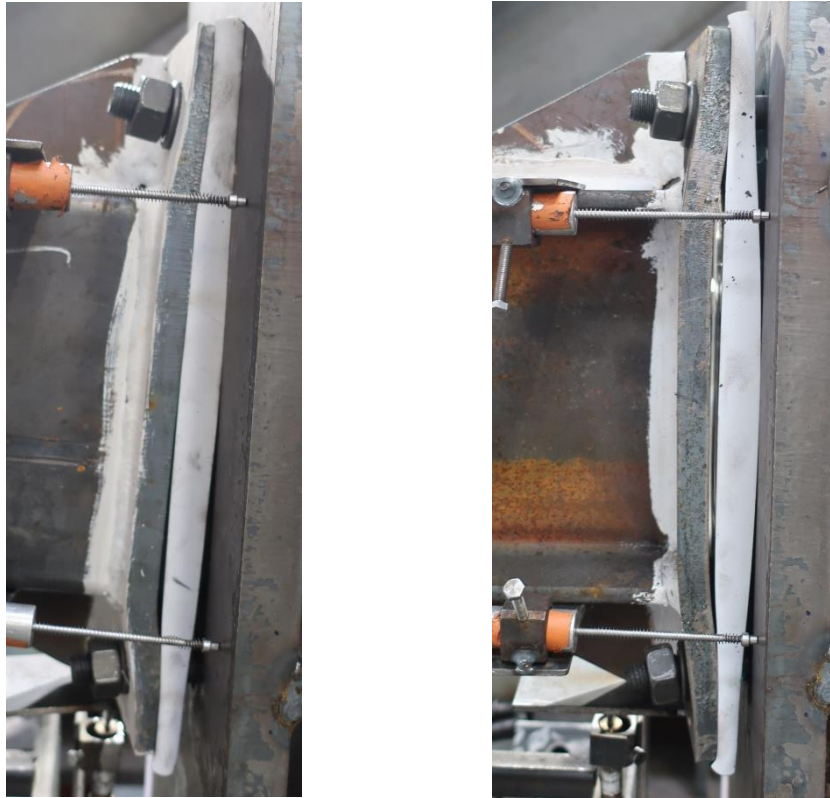
**Figure 20 – Deformed shape of specimens PA-1, RTPA-1-P/B at failure during cyclic test**

The maximum bending moment of specimen PA-2 obtained during cyclic test decrease by 10% comparatively to the monotonic test. The addition of a thermal insulation layer **does not** modify substantially the bending resistance and, as for the monotonic tests, a complete uplift of the flange is observed in the tensile area (see Figure 21-b, c and d).



*a- PA-2                      b- RTPA-2-P                      c- RTPA-2-P1                      d- RTPA-2-B*  
**Figure 21 – Deformed shape of specimens PA-2, RTPA-2-P/P1/B at failure during cyclic test**

For specimens with stiffeners and thermal insulation layer (specimens RTPA-4-P and RTPA-5-P), the maximum bending moment is increased during cyclic tests comparatively to monotonic one's. This can be explained by the fact that the crushing of the thermal insulation layer in compression eliminate the prying effect when tensile forces are applied to the bolt row and therefore limit bolt failure in tension. In contrast with specimens RTPA-1-P/B, the welds do not tear due to the presence of stiffeners and the lever arm between the beam and the bolts is maintained during the test.



*a- RTPA-4-P*

*b- RTPA-5-P*

**Figure 22** – *Deformed shape of extended end-plate during cyclic test*

#### *4.3.Moment-rotation curves*

The moment-rotation curves obtained during monotonic and cyclic loadings are superposed and presented in Figure 23. The monotonic curve envelopes cyclic curves except for specimen RTPA-5-P.

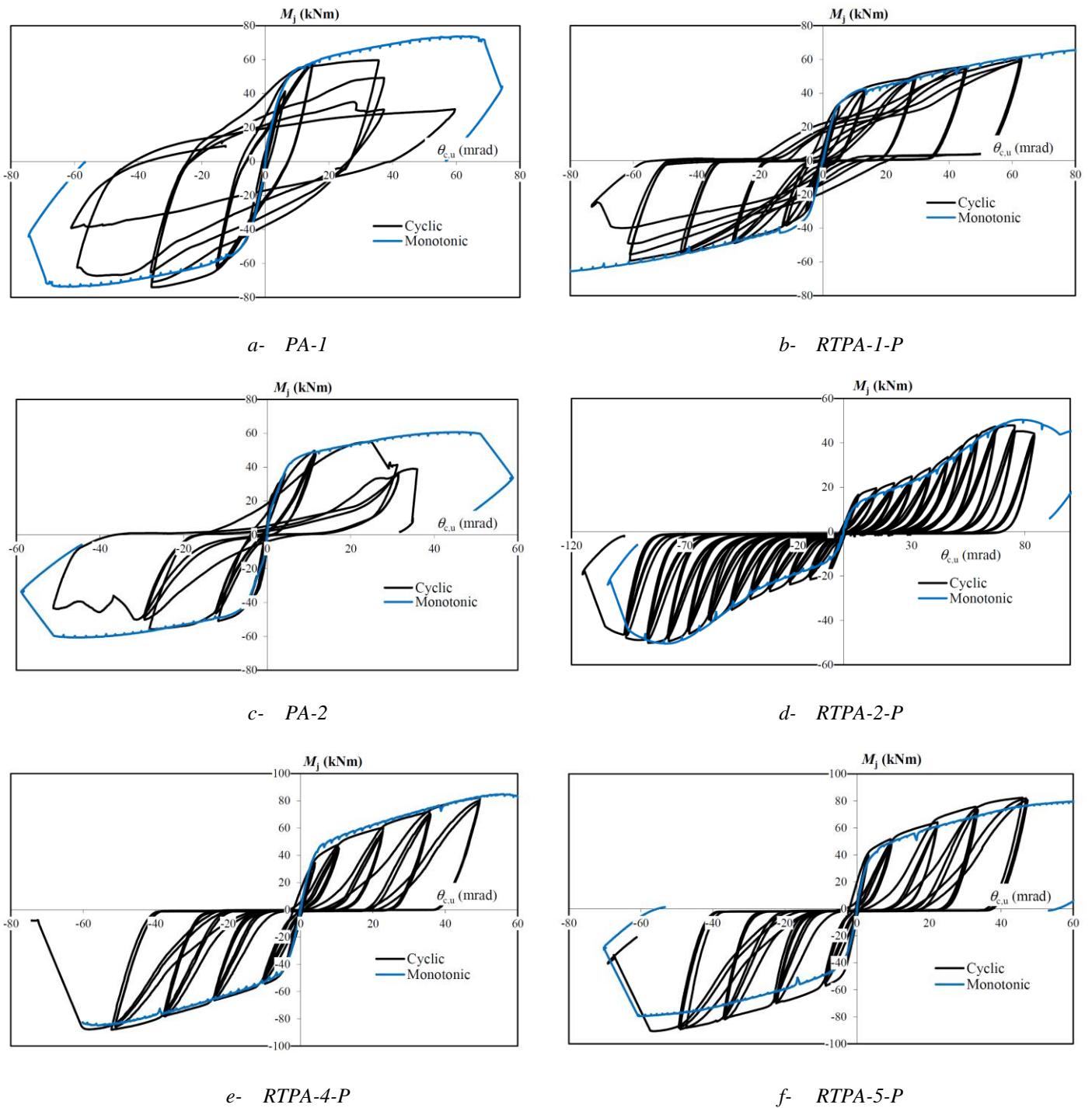


**Figure 23 – Moment-rotation curves during cyclic and monotonic tests**

For the two specimens tested without thermal insulation layer, PA-1 and PA-2, the ductility decreases during cyclic tests comparatively to monotonic one's. This drop is the result of premature failure of welds and bolts which are prone to low-cycle fatigue. For specimen RTPA-1-P, a decrease of rotation capacity is likewise observed as the failure mode is modified by the cycles. It goes from a bolt rupture (monotonic loading) to weld tearing followed by bolt failure (cyclic loading). The ductility of the other specimens is not substantially affected by cyclic loading. For specimens equipped

with thermal insulation layer and PA-2, cycles are generally characterized by a bending moment remaining equal to zero after unloading (see Figure 24). This pinching effect results from two gaps that develop in the connection:

- A first gap occurs between the end-plate and the support in the tensile area produced during the reverse loadings by permanent crushing of the insulation layer and yielding of the tensile components (end-plate in bending and/or bolts in tension).
- A second gap appears between the nut of the bolt and the end-plate in the compressive zone due to permanent insulating layer crushing. This phenomena is favoured at the end of the test by permanent bolt elongation.

These gaps should be closed just by a rigid body rotation of the end-plate (see Figure 21, Figure 22 and Figure 24), and thus the bending moment is close to zero during this stage. When the gap are closed the compressive and tensile forces can develop in the relative parts to equilibrate the bending moment. Specimen PA-1 is not affected by this phenomena as the outer edge of the flange is in contact with the column (see Figure 20-a) and compressive force can develop during unloading. The first stage during the unloading consist in closing the gap between the flange and the support by applying compressive forces.

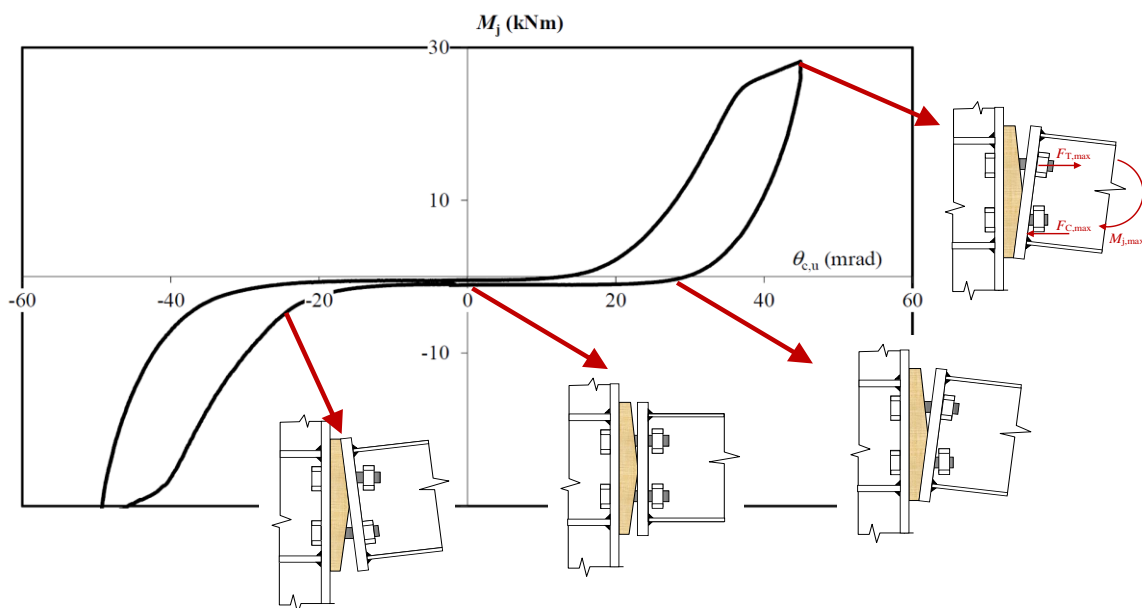


**Figure 24** – Pinching effect during a cycle of specimen RTPA-2-B

## 5 Conclusion

This paper give the results of an experimental campaign performed on beam to column bolted connection with intermediate thermal insulating layer. It consists in inserting a PVC or plywood plate between the end-plate of a steel beam and the steel member (column, beam, sleeve...). Cantilever beams attached to a steel column with thermal insulating layer were tested under monotonic and cyclic loadings and the main parameters studied were the material of insulation layer, the bolt configuration (flush end-plate, extended end-plate with and without stiffeners), the type of beam (I profile, RHS or SHS). From this experimental campaign, the following conclusions can be made:

- The addition of thermal insulating layer composed of PVC of 20 mm or plywood of 30 mm divide up to two the rotational stiffness of the extended end-plate comparatively to a conventional connection. For flush end-plate, this rotational stiffness is divided by 3 except when using a PVC layer of 10 mm thickness.
- The addition of thermal insulating layer increases the size of the compression area resulting in a reduction of the ultimate bending moment. This decrease is limited to 13% with extended end-plate and 20 % with flush end-plate. The failure modes were not modified when inserting a thermal insulating layer except for end-plate of RHS where weld tearing develops after major yielding of end-plate in bending.
- In presence of thermal insulating layer, the reduction of the plastic bending moment is more pronounced than that of the ultimate bending moment as the inelastic compression of the insulating layer occurs before the yielding of steel components (end-plate, bolt). For flush end-plate, the plastic bending moment is divided by 3 due to the limited size of the compression area which results in high stress level on the insulating layer.
- An extended end-plate with thermal insulating layer and stiffeners develops mechanical characteristics (rotational stiffness and bending resistances) similar to that of extended end-plate without thermal insulating layer and stiffeners.
- Since the thermal insulation layer is flexible, the compression area should extend to equilibrate the bending moment applied to the connection. Image correlation clearly permit to

highlight this phenomena. Thus in presence of extended end-plate with stiffeners and flush end-plate, the compression area extend over half the beam depth.

- The introduction of bolt preloading do not influence the rotational stiffness of the connection and the evolution of bolt force during loading is not affected by the level of bolt preloading.
- The failure mode obtained during cyclic loading is similar to that observed during monotonic loading. The resistance decreases in presence of extended un-stiffened end-plate but it is not necessarily the case with flush end-plate connections and particularly with extended stiffened end-plate. For the latter, prying effect disappear as the thermal insulating layer thickness reduces during the reverse loading.

The proposed solution with stiffeners limit effectively thermal bridges in steel structures and possess mechanical characteristics close to that of conventional connections without stiffeners. However, the long-term effect should be investigated in order to be able to estimate the evolution of the rotational stiffness that will influence greatly the displacement of the attached beam. Finally, an analytical model is under development to estimate the two main mechanical characteristics of this connection, the rotational stiffness and the bending resistances (plastic and ultimate). The assumption used classically concerning the position of the centre of compression cannot be retained as the compression area can extend over half the height of the connection and depend on the bolt arrangement.

### **Acknowledgments**

This research was partially funded by ADEME (Environnement and energy management Agency) with the contract ADEME n°1704C0003. The project consortium is composed of CTICM, INSA Rennes and PERRAUD.

## 6 References

- [1] Hardock D. and Roppel P., Thermal Breaks and Energy Performance in High-rise Concrete Balconies, CTBUH Journal, Issue IV, 2013, pp. 32-37.
- [2] Keo P., Le Gac B., Somja H., Palas F., Experimental study of the behavior of a steel concrete hybrid thermal break system under vertical actions. High tech concrete: where technology and engineering meet. Springer; 2018. p. 2573–80.
- [3] Keo P., Le Gac B., Somja H., Palas F., Low-cycle fatigue life of a thermal break system under climatic actions, Engineering Structures, Vol. 168, p.525-543, 2018.
- [4] Nasdala L., Hohn B., Rühl R., Design of end-plate connections with elastomeric intermediate layer, Journal of Constructional Steel Research, Vol. 63, p. 494-504, 2007.
- [5] Sulcova Z., Sokol Z., Wald F., Structural connections with thermal separation, CESB 07 Prague Conference, p.672-677, 2007.
- [6] Cleary D.B., Riddell W.T., Camishion N., Downey P., Marko S., Neville G., Oostdyk M., Panaro T., Steel connections with fiber-reinforced resin thermal barrier filler plates under service loading, Journal of Structural Engineering, Vol. 142, Issue 11, 2016.
- [7] Peterman K.D., Moradei J., D’Aloisio J., Webster M., Hajjar J.F., The behaviour of double lap splice bolted connections with fiber-reinforced polymer fills, Workshop Connection VIII, Boston, May 2016.
- [8] K. D. Peterman, J. A. Kordas, J. Moradei, K. Coleman, J. A. D’Aloisio, M. D. Webster, and J. F. Hajjar, “Thermal Break Strategies for Cladding Systems in Building Structures: Report to the Charles Pankow Foundation,” Boston, MA, 2016.
- [9] Ben Larbi A., Couchaux M., Bouchaïr A., Thermal and mechanical analysis of thermal break with end-plate for attached steel structures, Engineering Structures, Vol. 131, p. 362-379, 2017.

- [10] Hamel S., White S., Thermo-mechanical modelling and testing of thermal breaks in structural steel point transmittances, Anchorage, AK, 2016.
- [11] Shi G., Shi Y., Wang Y., Behaviour of end-plate moment connections under earthquake loading, *Engineering Structures*, Vol. 29, p.703-716, 2007.
- [12] Broderick BM, Thomson AW. The response of flush end-plate joints under earthquake loading. *Journal of Constructional Steel Research* 2002; 58(9):1161–75.
- [13] Swanson JA, Leon RT. Bolted steel connections: tests on T-stub components. *Journal of Structural Engineering*, Vol. 126, No. 1, p.50–56, 2000.
- [14] Piluso V., Rizzano G., Experimental analysis and modelling of bolted T-stubs under cyclic loads, *Journal of Constructional Steel Research*, Vol. 64, p.655-669, 2008.
- [15] EN 1993-1-8, Eurocode 3: Design of steel structures. Part 1-8: Design of joints, 2005.
- [16] NF EN 1090: Execution of steel structures and aluminium structures, Part 2: Technical requirements for steel structures, CEN, February 2009.
- [17] ECCS, Recommended testing procedures for assessing the behavior of structural elements under cyclic loads, European Convention for Constructional Steelwork, Technical Committee 1, TWG 13 – Seismic Design, No45, 1986.